SUPPORTING INFORMATION

Functional Imaging Reveals Rapid Reorganization of Cortical Activity after Parietal Inactivation in Monkeys

Melanie Wilke*, Igor Kagan* and Richard A. Andersen

Supporting information contains:

7 Supporting Figures

7 Supporting Tables

Supporting Methods

Abbreviations

Supporting References

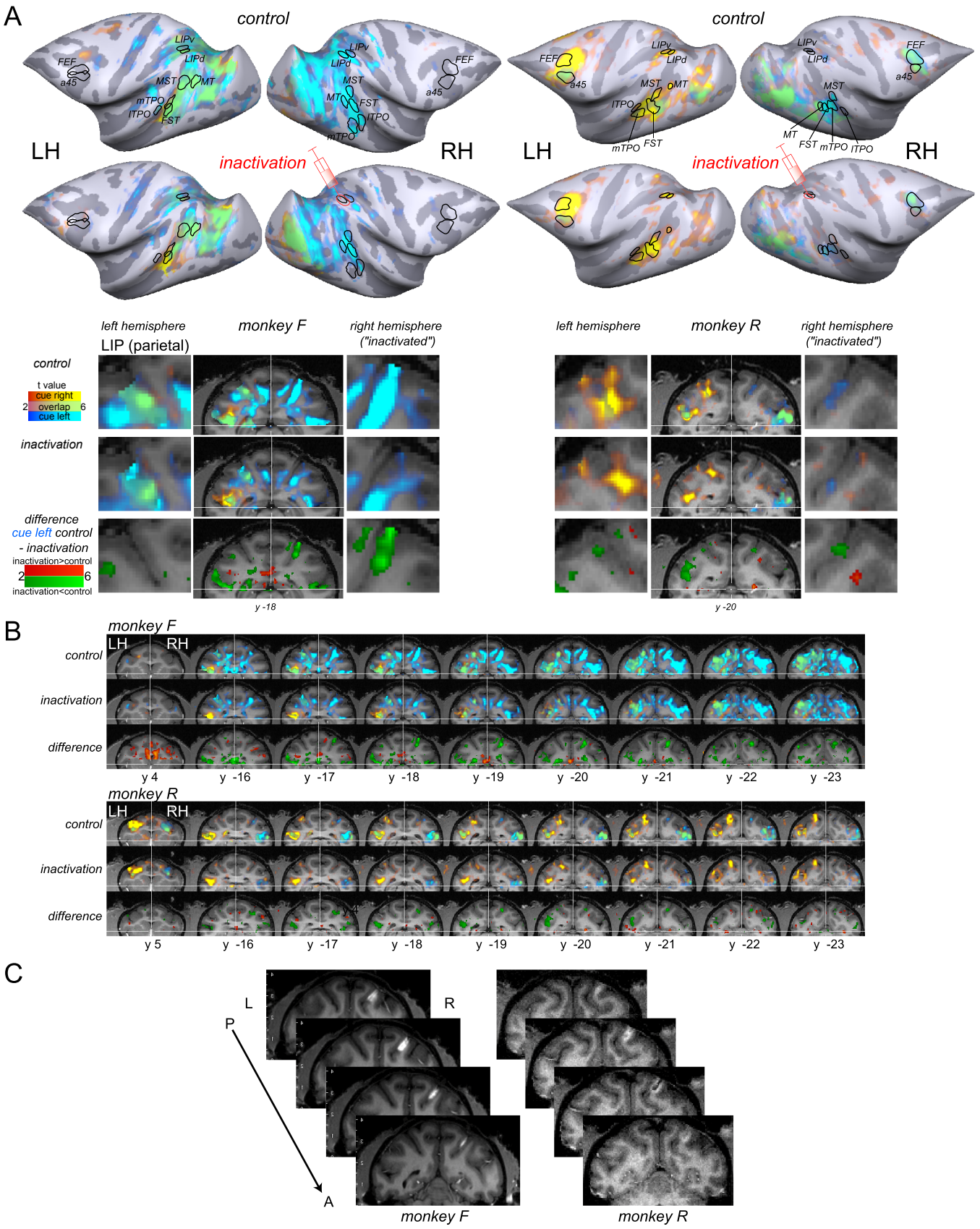

Fig. S1. BOLD activity changes in instructed trials, and injection locations. *(A)* (Upper) Superimposed activity maps for instructed +cue left and +cue right contrasts in control (upper row) and inactivation (lower row) sessions. Note the reduction of contralesional (left) cue activity after inactivation of right LIP, expressed as a "diminished" spread/intensity of cyan-blue maps. Here and in (B): color scale: t-values (from 2 to 6), intensity scales with significance. RH - right hemisphere (inactivated); LH - left hemisphere. Black contours - area outlines of volume ROIs used for ERA analyses, red contours - outlines of injection volume. Since the surface maps do not reveal the activity above or below the surface boundary (e.g. within sulcal gray matter), example coronal sections are shown below and in Fig. S2. (Lower) Superimposed activity maps for +cue left and +cue right contrast (first two rows in each panel), and contralesional cue left "control minus inactivation" difference (third row) in example coronal sections through ips and sts, with enlarged maps showing LIP. Inactivation effects on contralesional cue activity can be seen as diminished cyan-blue clusters and as green clusters in the difference maps. Note the activity decrease around the injection side. *(B)* Additional coronal sections showing superimposed activity maps for instructed +cue left and +cue right contrasts in control (upper row) and inactivation (lower row) sessions for monkeys F and R. Third row depicts the cue left control - inactivation activity difference. Anterior-posterior (y) coordinates are in AC-PC plane. *(C)* Four consecutive coronal slices through the inactivation site, inter-slice interval 1 mm. Monkey F - 4 μl injection; monkey R - 4.5 μl injection.

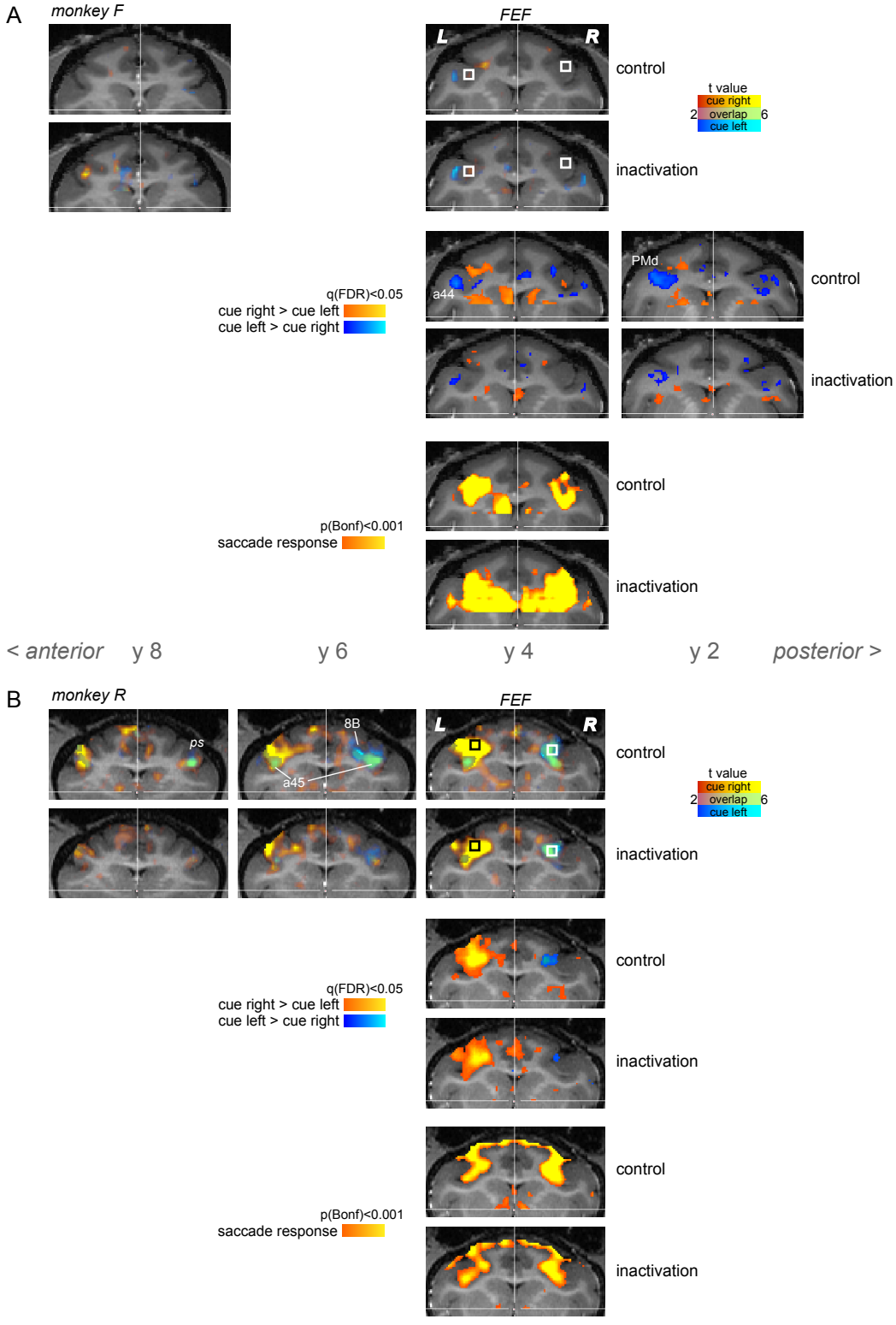

Fig. S2. BOLD activity changes in instructed trials in frontal regions. Coronal sections showing activity in FEF, a45 and in neighboring areas in instructed trials in control and inactivation sessions. FEF ROIs are denoted by small black and white squares. *(A)* Monkey F. Due to the usage of the surface quadrature coil in monkey F, he showed very weak cue/delay activation (relative to the fixation baseline) in FEF and a45 (top two rows). The FEF and a45 ROI amplitudes showed contralesional cue increase in the left hemisphere after inactivation, which was not apparent in the maps, because the "positive" cue activation did not reach a significance threshold (min t value 2). To inspect inactivation consequences regardless of the response amplitude relative to the fixation baseline, we plotted *cue right* > *cue left* (yellow-red) and *cue left* < *cue right* (cyan-blue) maps before and after inactivation (middle two rows). These maps show a decrease of contralesional (left>right) tuning in the left hemisphere in the ventral bank of lower arcuate sulcus (area a44?) and more posterior from FEF in area PMd (y=2 section) in the arcuate spur (less cyan-blue voxels). The activation by saccades (used to extract FEF ROIs in monkey F) is more pronounced and is shown in the bottom two rows. *(B)* Monkey R. The consequence of LIP inactivation was mainly a decrease of responses to contralesional single targets (less cyan-blue), in the area a45 in the lower limb of arcuate sulcus; more anterior to the main FEF locus, in area 8B in the upper limb of arcuate sulcus (y=6 section), and in the principle sulcus (ps, y=8 section). There was also some decrease of ipsilesional responses (less yellow-orange voxels). As shown in Fig. 4, there was no statistically-significant change in response amplitudes extracted from the FEF and a45 ROIs.

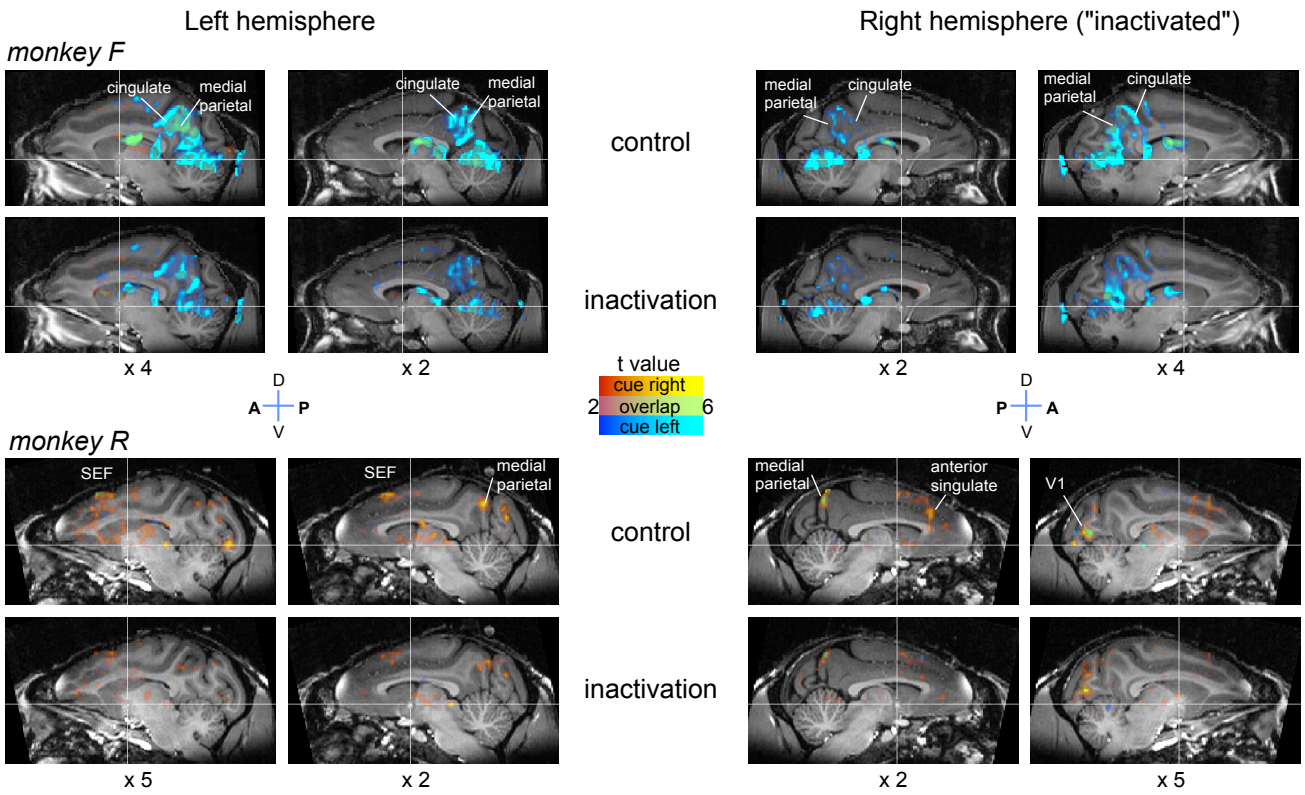

Fig. S3. BOLD activity changes in instructed trials in the medial aspect of cortical hemispheres. Sagittal sections showing activity in medial parietal and cingulate cortices and supplementary eye fields (SEF) in instructed trials in control and inactivation sessions. In monkey F (top), left cues (cyan-blue voxels) caused stronger activation than right cues (yellow-red voxels). In monkey R (bottom), the situation was opposite: right cues (yellow-red voxels) caused stronger activation than left cues in control sessions. In both monkeys, the inactivation reduced the intensity of responses to both contralesional (left) and ipsilesional (right) cues, however the contralesional effect was more pronounced, therefore the effect was more apparent in monkey F.

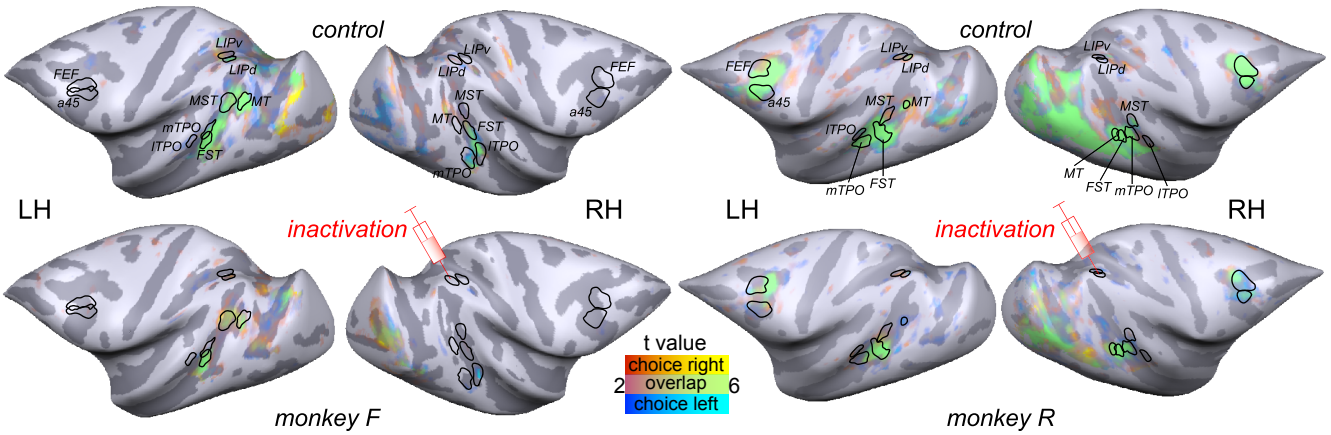

Fig. S4. Inactivation effects on cue/delay activity in choice trials. Superimposed activity maps for +choice left (yellow-red) and + choice right (cyan-blue) contrasts in control (upper row) and inactivation (lower row) sessions. Same conventions as in Fig. S1A. Most areas responded nearly equally to bilateral targets, as evidenced by largely overlapping activity patterns (green). Color scale denotes t-values (from 2 to 6), intensity scales with significance. RH - right hemisphere (inactivated); LH - left hemisphere.

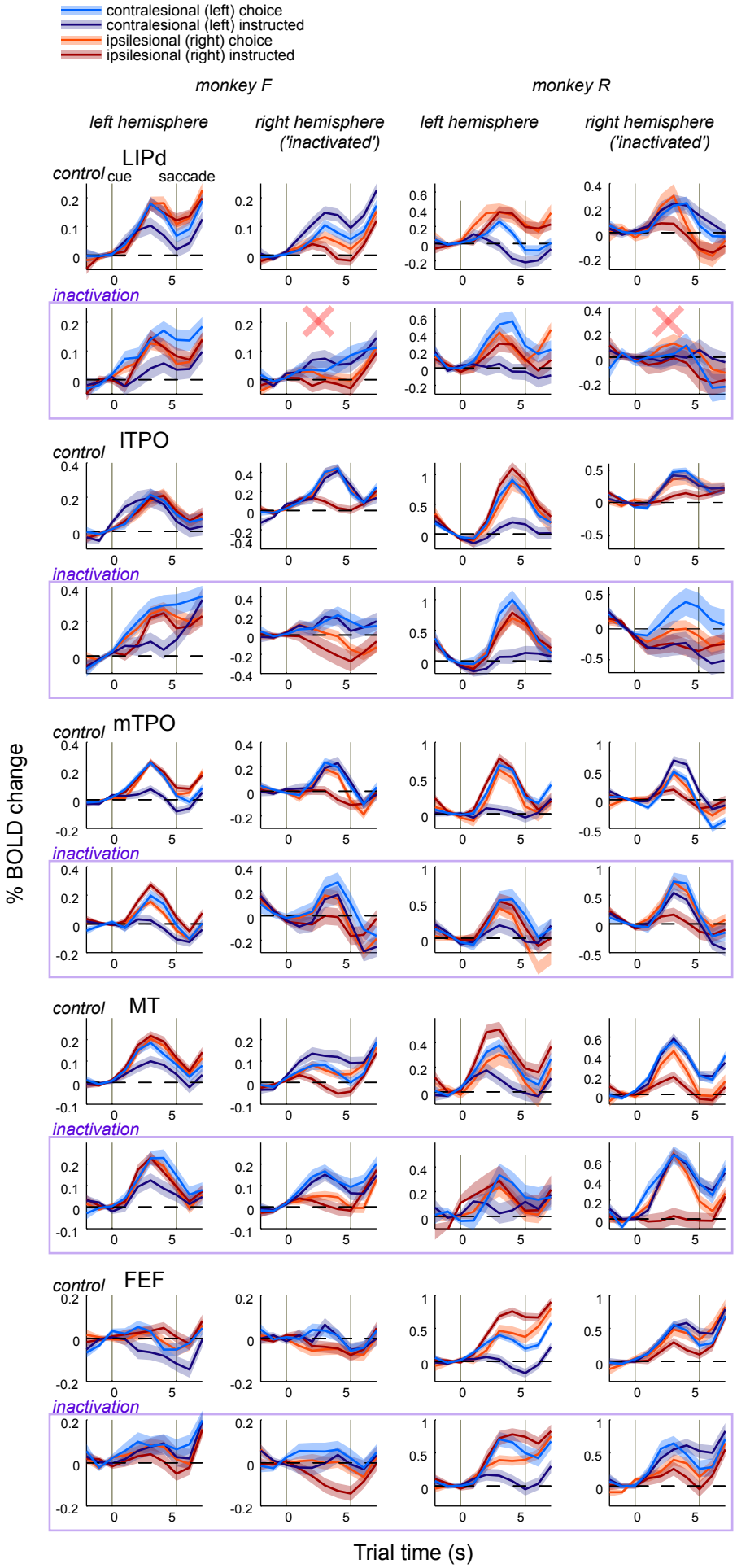

Fig. S5. Time-courses in instructed and choice trials for areas LIPd, mTPO, lTPO, MT and FEF. ERA time-courses for all 4 trial types (left and right instructed, left and right choice) in control and inactivation sessions, aligned to the 200 ms cue offset (0 s). Shaded error bands indicate s.e.m. across trials. Note the increase of cue/delay activity for contralesional (left, light blue) choice trials relative to ipsilesional (right, orange) choice trials, present in both hemispheres (mTPO, lTPO and FEF, both monkeys; MT, monkey F), and in the intact hemisphere (LIPd, both monkeys), after inactivation.

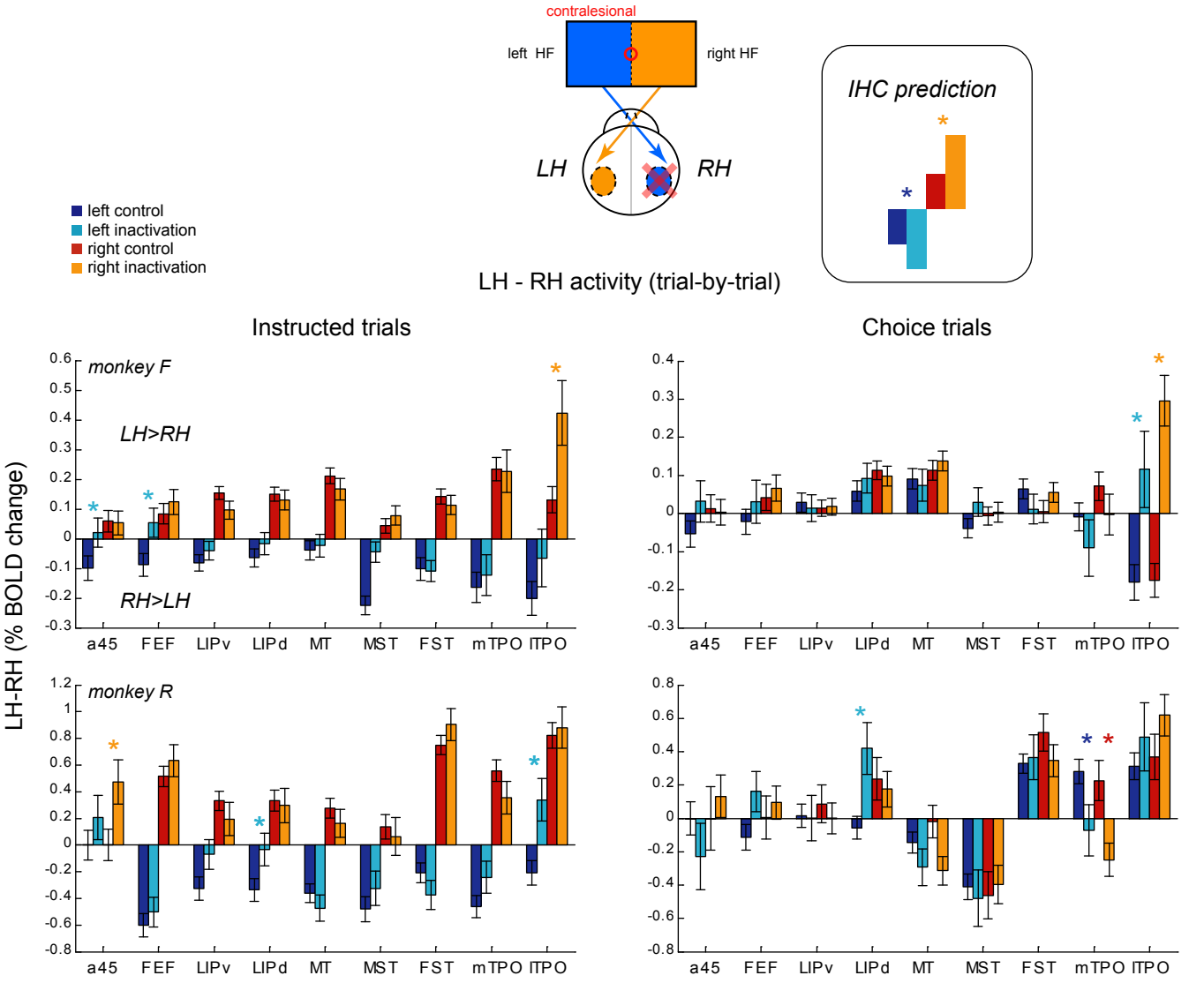

Fig. S6. Left hemisphere - right hemisphere (LH - RH) %BOLD response change. In the formulation of the interhemispheric competition model, RH inactivation should lead to more activity in LH (intact hemisphere) and less activity in RH, and thus increased LH-RH difference, for the ipsilesional choices, and conversely, LH-RH decrease for contralesional choices (see inset on the right). None of the bilateral ROI pairs fulfilled this prediction - instead, area ITPO showed increase for both choices (significant in monkey F, with the same trend in monkey R), mTPO showed decrease for both choices, and LIPd in monkey R showed increase for contralesional choice (probably reflecting a compensation in the intact LH).

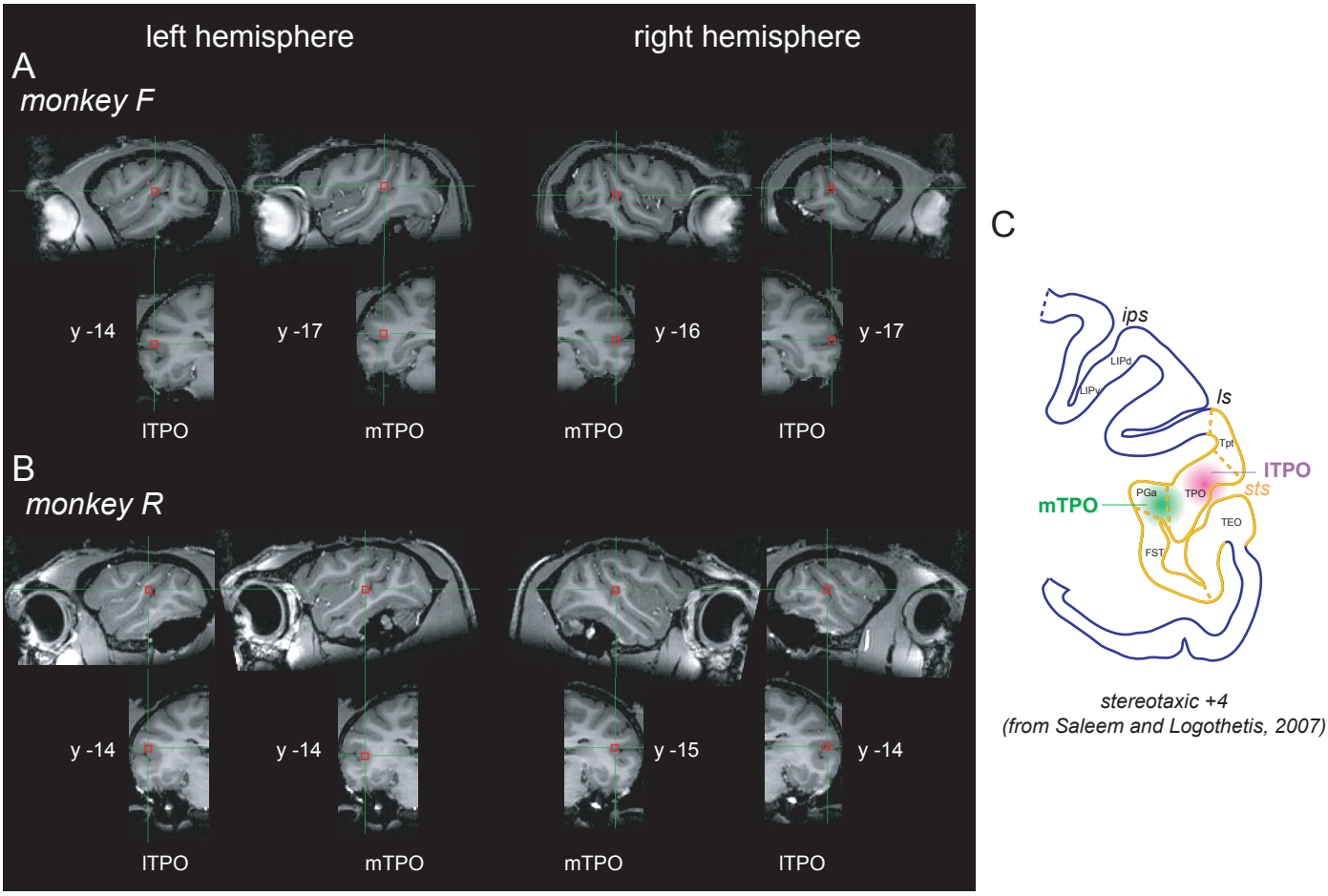

Fig. S7. *(A)* Monkey F, (top) sagittal sections through sts showing location of coronal sections (bottom) through medial TPO (mTPO) and lateral TPO (lTPO), separately for each hemisphere. In each panel, green cross-hair denotes the center of 2.53 mm ROI selection (red box). *(B)* Monkey R, same conventions as in (A). *(C)* Schematic illustration of the anatomical locations assigned to lTPO and mTPO ROIs, derived from the monkey brain atlas of Saleem and Logothetis, stereotaxic +4 coronal section. Abbreviations: FST, fundus of superior temporal sulcus; *ips*, intraparietal sulcus; *ls*, lateral sulcus; LIPd, lateral intraparietal area, dorsal; LIPv, lateral intraparietal area, ventral; *sts*, superior temporal sulcus; lTPO, area TPO in the lateral portion of sts dorsal bank; mTPO, area TPO in the medial portion of *sts* dorsal bank (overlapping with area PGa); Tpt, temporo-parietal area; TEO, area TEO (ventral bank of sts).

Supporting Tables

List of Supporting Tables

S1: Injection volume and behavioral effects per session.

S2: Effect of gadolinium injection on local LIP activity.

S3: Coordinates of ROIs used in ROI analysis.

S4: Number of trials used for ERA analysis, per condition, and number of functional runs.

S5: ROI analysis: effects of inactivation on BOLD activity in instructed trials.

S6: ROI analysis: effects of inactivation on BOLD activity in choice trials.

S7: ROI analysis: effects of inactivation on BOLD activity in choice trials - relative signal difference between left and right choices.

monkey F		*% ispilesional choices*	***monkey R***		*% ispilesional choices*
Inactivation session	***Volume (μl)***		***Inactivation session***	***Volume (μl)***	
20081107	2.5	68.7	20090930	2.5	63.7
20081110	3.0	84.1	20091002	2.5	55.3
20081112	3.0	58.4	20091006	5.0	66.6
20081125	3.0	58.6	20091215	4.5	80.6
20081217	5.0	79.9	20091217	4.5	53.8
20081221	5.0	63.6			
Control session			***Control session***		
20081029	-	56.3	20090928	-	36.4
20081105	-	41.0	20091001	-	36.3
20081114	-	34.4	20091004	-	28.9
20081119	-	34.6	20091216	-	31.5
20081121	-	64.1	20091221	-	11.7
20081212	-	41.7			
Gadolinium only					
20081105	4.0	41.0			
20090107	3.0	18.5			
20090304	4.0	39.4			

Table S1. Injection volume and behavioral effects (*% ipsilesional choices*) in monkeys F and R as a function of session (listed chronologically from first to last for each condition separately; control and inactivation sessions were interleaved).

Condition	*Cue/delay response, %BOLD change*		*Saccade response, %BOLD change*	
	LIPv	*LIPd*	*LIPv*	*LIPd*
Control (no injection)	0.12	0.13	0.33	0.29
Gadolinium only	0.07 ($p = 0.21$)	0.08 ($p = 0.2$)	0.27 ($p = 0.12$)	0.24 ($p = 0.12$)
Muscimol + Gadolinium	0.09 ($p = 0.52$)	0.06 ($p = 0.07$)	0.19 ($p < 0.01$)	0.2 ($p < 0.05$)

Table S2. Effect of gadolinium injection on local LIP activity: contralesional cue/delay and saccade BOLD responses in the vicinity of injection sites, in monkey F (right hemisphere). Note the response amplitude decrease in gadolinium only condition, suggesting tissue perturbation and/or susceptibility artifacts. Nonetheless, the decrease was more pronounced and only reached statistical significance when muscimol was co-injected. P-values were derived from a two-tailed t-test (control vs. gadolinium only or control vs. muscimol + gadolinium, respectively).

Cortical area	*Left ROI*			*Right ROI*		
	x	***y***	***z***	***x***	***y***	***z***
a45	-16	6	10	15	4	9
	-16	6	9	13	6	9
FEF	-15	5	11	15	3	13
	-12	4	13	11	5	12
LIPv	-10	-19	14	10	-19	14
	-9	-21	16	10	-21	17
LIPd	-11	-20	17	9	-22	18
	-7	-22	19	11	-20	19
MT	-21	-23	12	21	-21	7
	-17	-25	9	23	-19	5
MST	-17	-20	9	14	-20	7
	-16	-20	8	23	-18	7
FST	-20	-17	3	17	-19	4
	-20	-18	4	21	-19	3
mTPO	-21	-17	5	21	-16	2
	-20	-14	2	20	-15	4
lTPO	-25	-14	4	25	-17	3
	-23	-14	5	24	-13	4

Table S3. Cue-activated areas and coordinates for left and right ROIs in AC–PC bicommissural space. For each area entry, the upper row is for monkey F, and the lower row is for monkey R.

	Monkey F			***Monkey R***	
Condition	*Control*	*Inactivation*	*Gad. only*	*Control*	*Inactivation*
Instructed left	275	181	134	250	117
Instructed right	415	278	181	264	107
Choice left	358	167	218	385	90
Choice right	379	387	103	111	154
N runs (20 min each)	**42**	**30**	**20**	**33**	**17**

Table S4. Numbers of trials for each condition used for ERA analysis (correct trials without excessive head/body motion) and number of functional runs (each run 20 min, 1200 volumes with TR 1 s) in monkeys F and R.

monkey F instructed										
		a45	FEF	LIPv	LIPd	MT	MST	FST	mTPO	lTPO
LH	Right (ipsilesional)	0.95	0.48	0.99	0.33	0.74	0.65	0.99	0.82	0.5
LH	Left (contralesional)	**0.04**	**0.01**	0.63	0.65	0.7	0.02	0.76	0.34	0.38
RH	Right (ipsilesional)	0.84	0.1	0.04	0.63	0.36	0.6	0.42	0.98	**0.01**
RH	Left (contralesional	0.92	0.85	0.52	0.07	1.0	0.09	0.88	0.36	**0.04**
monkey R instructed										
		a45	FEF	LIPv	LIPd	MT	MST	FST	mTPO	lTPO
LH	Right (ipsilesional)	0.1	0.7	0.3	0.48	0.08	0.46	0.62	0.11	0.09
LH	Left (contralesional	0.23	0.2	0.87	0.27	0.82	0.71	0.72	0.52	0.69
RH	Right (ipsilesional)	0.23	0.55	0.8	0.66	0.5	0.97	0.34	0.93	**0.01**
RH	Left (contralesional	0.94	0.71	0.04	0.1	0.12	0.41	0.19	0.28	**0.0**

Table S5. ROI analysis: effects of inactivation on BOLD activity in instructed trials. P-values from two-tailed unpaired t-test comparing single trial cue/delay BOLD response amplitudes between control and inactivation conditions in same ROIs, separately for each hemisphere and for each monkey. LH/RH – left/right hemisphere, right/left – right/left hemifield cues. Values $p<0.05$ are marked by **bold font** (blue is for contralesional cues, orange for ipsilesional cues).

monkey F choice										
		a45	FEF	LIPv	LIPd	MT	MST	FST	mTPO	lTPO
LH	Right (ipsilesional)	0.76	0.07	0.56	0.09	0.73	0.48	0.95	**0.01**	0.18
LH	Left (contralesional)	**0.01**	0.06	0.98	0.65	0.12	0.09	0.66	0.35	0.09
RH	Right (ipsilesional)	0.58	0.21	0.62	0.16	0.66	0.63	0.12	0.79	**0**
RH	Left (contralesional	0.33	0.34	0.65	0.69	**0.04**	0.97	0.40	0.60	0.05
monkey R choice										
		a45	FEF	LIPv	LIPd	MT	MST	FST	mTPO	lTPO
LH	Right (ipsilesional)	0.59	0.79	0.59	0.63	0.5	0.94	0.67	0.19	0.50
LH	Left (contralesional)	0.95	**0.01**	0.67	**0**	0.97	0.63	0.28	0.73	0.64
RH	Right (ipsilesional)	0.2	0.36	0.87	1.0	**0.03**	0.75	**0.02**	**0.04**	**0.02**
RH	Left (contralesional	0.14	0.75	0.61	0.18	0.09	0.44	0.28	**0.03**	0.52

Table S6. ROI analysis: effects of inactivation on BOLD activity in choice trials. P-values from two-tailed unpaired t-test comparing single trial cue/delay BOLD response amplitudes between control and inactivation conditions in same ROIs, separately for each hemisphere and for each monkey. LH/RH – left/right hemisphere, right/left – right/left hemifield choices. Values $p<0.05$ are marked by **bold font**.

monkey F choice *(per session, 15 trials minimum)*									
	a45	FEF	LIPv	LIPd	MT	MST	FST	mTPO	lTPO
LH	**0.03**	0.26	0.79	0.13	**0**.44	0.29	0.83	0.47	0.32
RH	0.25	0.25	0.54	0.4	**0.01**	0.82	0.09	0.41	**0.03**
monkey R choice *(per session, 5 trial minimum)*									
	a45	FEF	LIPv	LIPd	MT	MST	FST	mTPO	lTPO
LH	0.23	**0.01**	0.2	**0.03**	0.37	0.57	0.14	0.44	0.48
RH	**0.01**	**0.01**	0.1	0.73	0.54	0.33	0.71	0.53	**0.03**

Table S7. ROI analysis: effects of inactivation on BOLD activity in choice trials – relative signal difference between contralesional (left) and ipsilesional (right) choices. P-values from two-tailed (control<inactivation) unpaired t-test comparing, across all sessions in both monkeys, mean left-right choice difference of cue/delay fMRI response amplitude, between control and inactivation conditions in same ROIs, separately for each hemisphere. LH/RH – left/right hemisphere. Values $p<0.05$ are marked by **bold font**.

Supporting Methods

Experimental preparation

Two male rhesus macaques (*Macaca mulatta*) weighting 8-10 kg were implanted with a MR-compatible plastic (PEEK) headpost embedded in Palacos bone cement (BioMet) attached to the cranium with short ceramic screws (Thomas Recording), under general anesthesia. Monkeys were chronically implanted with a 23 gauge guide PEEK cannula (Plastics One, VA) penetrating the dura and targeting the lateral bank of the *ips* (LIP) in the right hemisphere. A small hole was drilled into the skull, exposing ~3 mm of dura, a penetration was made by means of a guide needle, and the cannula was lowered into the brain using a stereotaxic holder. The cannula was embedded in a corrugated ceramic cylinder, which was affixed to the skull with ceramic screws (Thomas Recording) and dental acrylic. This chronically implanted outer cannula served as a guide for inserting a 28 gauge internal PEEK cannula during the experiments. Cannulae placement and trajectory were guided by transforming a pre-surgical T1-weighted high-resolution structural MRI into the stereotaxic plane.

MR imaging

Monkeys were scanned in a Bruker Biospec 4.7T/60cm vertical bore scanner equipped with a BGA38S2 gradient coil using a ParaVision 4.0. A linear birdcage volume RF coil (monkey R) or a quadrature surface RF coil (monkey F) allowed whole head coverage (Bruker). First- and second-order shimming of the B0 field was performed with the FASTMAP algorithm. Functional images were collected with a BOLD-sensitive T2*-weighted GE-EPI single-shot sequence using TR 1 s, TE 20 ms, 60° flip angle, 200kHz bandwidth, 96x96 matrix, 12.8 cm FoV, 1.33x1.33 mm in-plane resolution and 14 2 mm oblique (15°) continuous slices. EPI distortions in phase-encoded dimensions were corrected using PLACE EPI sequence (1). For registrations with EPI, in-plane structural images were obtained using T1-weighted MDEFT-RAGE during each session; a whole-head high-resolution (0.5 mm^3) scan was obtained in a separate session.

Pharmacological inactivation

Microinfusions of GABA-A agonist muscimol (Tocris Bioscience, MO) were made in each inactivation session via a sterile 28 gauge internal cannula. To confirm the injection locations, the MR contrast agent gadolinium (Magnevist; Berlex Imaging, NJ) was added to the solution of weak

phosphate buffered saline and anatomical MR images were acquired. The muscimol was dissolved in PBS (along with the gadolinium), and the solution (pH 7.0-7.5) was sterile filtered (Corning Inc., NY) prior to injection. Specificity of drug effects was validated in 3 control sessions in which only the vehicle and gadolinium were injected. Total injection volumes ranged from 2.5-5.0 µl of 6.6 mg/ml and were delivered at a rate of 0.5-1.0 µl/min using a 100 µl gas-tight Hamilton syringe driven by a digital infusion pump (Harvard Apparatus, MA). BOLD activity was measured during the time interval in which behavioral effects were present, typically between 40 – 180 min after the injection. To maintain a steady level of behavioral effect across sessions, we gradually increased the injection volume from 2.5 µl to 5 µl (**Table S1**). We conducted 8 inactivation sessions in monkey F and 5 inactivation sessions in monkey R. Two out of 8 inactivation sessions in monkey F in which we used the same drug solution did not show any behavioral effect. Since there was the suspicion that the lack of behavioral effects was due to the age of the drug solution and since we were interested in studying the neural underpinning of the choice bias, we excluded those sessions from the fMRI analysis. In total, we further analyzed 6 inactivation and 6 control sessions without injection in monkey F, and 5 inactivation and 5 control sessions in monkey R, plus 3 additional control sessions in monkey F during which we injected gadolinium without the muscimol. Trial numbers for each monkey/condition are shown in **Table S4**.

Stimulus presentation, online behavioral control and data acquisition

Visual stimuli were presented on 800x600@60 Hz LCD goggles (Resonance Technology) subtending 30x24° of visual angle using custom OpenGL software. Eye position was monitored at 60 Hz and 0.5-1° accuracy with an MR-compatible mini-IR camera (Resonance Technology / Arrington Research) and recorded together with stimulus and timing information and TTL triggers from the scanner. Online behavioral control and feedback were implemented in a LabVIEW RT (National Instruments). Incorrect trials were aborted; successful trials were rewarded with a 0.5-1 ml water drop. The visual cues were randomly chosen from 18 (10°-16°) locations, 9 in the left and 9 in the right visual hemifield. Video-based motion detection systems were used to train the monkeys to minimize their body, limb and jaw motions, and to track their behavior during scanning. Trials compromised by motion were aborted and punished with a time-out during training and scanning (2).

Data analysis

Functional data were analyzed in BrainVoyager QX and MATLAB running on a Fedora Core 5 (64 bit) Linux. All trial events: cue, memory delay, saccade, reward delivery and inter-trial interval (except initial fixation period that served as the baseline epoch) – were extracted and used as predictors for the general linear model (GLM) after convolution with the monkey hemodynamic response function (HRF), which we found to be faster than the standard human HRF (2). Events from all trials (successful and failed) were modeled to account for the overall variance. Each session was first analyzed separately and, as findings were consistent across sessions, control and inactivation sessions were combined using multi-session GLM. Areas were identified by matching the individual sulcal patterns to the macaque atlas (3). ROIs were defined in each subject using event-related maps for contralateral +cue contrasts, which identified clusters active during the task, aided by the localization to individual sulcal patterns, referenced to the macaque brain atlas (3). Based on the atlas, we further subdivided area TPO into lateral and medial parts (lTPO and mTPO). Area mTPO roughly corresponds to area PGa, while lTPO is adjacent to area Tpt (**Fig. S7**). For the BOLD time-course event-related averaging (ERA), only successful trials were accumulated. Selection of successful trials ensured that activity would not be affected by signals from incomplete trials. Epochs affected by body or limb motions were automatically detected and eliminated from ERA analysis.

Time-courses were constructed using individual baseline estimates for each single trial: mean activity in the last 2 s of the initial fixation period ("epoch-based" averaging in BrainVoyager). The typical ERA time-course (%BOLD change relative to fixation period baseline, as a function of trial time) is shown in **Figure 1C**. The initial signal is due to eye movements and resultant visual stimulation in the preceding inter-trial interval (ITI) and fixation point acquisition at time 0 s. During the 6.8 s fixation period, the signal decreased and returned to a baseline, and a brief cue (200 ms) was presented unilaterally (instructed trials) or bilaterally (choice trials). The first peak after the cue presentation is due to cue and delay period activity, the second, usually stronger, peak and subsequent activation in the end of the trial is due to saccade response and unconstrained eye movements in waiting for reward, reward and ITI intervals. To quantify the time-courses, we estimated the mean response amplitude in a 3 s cue/delay interval for each trial type (**Fig. 1C**).

Functional data preprocessing

The first 4 EPI volumes were excluded from functional analyses to remove transient effects of magnetic saturation, but were used for co-registration, since they provide better contrast for anatomical landmarks. PLACE-undistorted EPI sequences for each run were preprocessed using slice time correction, linear trend removal and a high-pass temporal filter with 3 cycles per 20 min run cut-off, and 3D-aligned to the first volume of the first run in the session using 6 degrees of freedom. The in-plane T1-weighted anatomical scan for each separate session was co-registered to the high-resolution structural scan in the AC-PC plane, and then EPI runs were aligned to the AC-PC-registered anatomical scan using rigid body transformations. Automated alignment procedures were followed by careful visual inspection and manual fine-tuning based on anatomical landmarks. Using these transformations, 4D volume time-courses (VTC) were computed in AC-PC space using 1x1x1 mm voxel size and a 1000 unit image intensity threshold (mean image intensity within the brain ranged from 4000 to 6000 units). No additional spatial smoothing was applied to the fMRI data. The statistical contrast maps were upsampled (interpolated) to a 0.5^3 mm resolution of anatomical scans.

Local effects of inactivation

Besides the actual inhibiting effect of muscimol on the neuronal activity, the decrease of the fMRI signal in LIP can be partially attributed to gadolinium-induced local magnetic susceptibility. To quantify this, we performed 3 additional sessions in monkey F in which we injected only gadolinium solution without muscimol. The injection of gadolinium led to a decrease of fMRI signal in LIP, but the effect was weaker than with muscimol, suggesting that the local fMRI activity decrease was mainly due to the muscimol suppression of neuronal firing (**Table S2**).

ROI selection procedure

ROI selection was based on the control sessions activation maps for "+contralateral cue" contrast: "+rightward cues - initial fixation baseline" for left hemisphere ROIs, and "+leftward cues - initial fixation baseline" for right hemisphere ROIs, using q(FDR) = 0.01 or q(FDR) = 0.05 (FDR: False Discovery Rate correction for multiple comparisons). In most cortical areas, these statistical activations maps were more extensive than 2.5^3 mm ROIs we used; thus we selected the ROIs based on the conjunction of maximal activation with an individual sulcal/gyral pattern of underlying high-resolution MRI, matching it to the areas as delineated in the Saleem and

Logothetis atlas (3). All ROI time-course extraction was done from the volume (3D) data, not from the surface maps. The surface maps show the activity patterns at the reconstructed boundary in the middle of gray matter thickness, therefore some of the volume activation above and below this boundary may not be visible on in the surface maps.

Selection of frontal ROIs in monkey F

The exception to the procedure of selecting ROIs based on the contralateral cue contrast (i.e. "+cue left" or "+cue right") was the selection of frontal ROIs a45 and FEF in monkey F. In these areas, there was almost no "positive activation" for the cue response, relative to the fixation baseline. However, the inspection of the ERA time-courses from these regions extracted on the basis of saccade activation map (**Fig. 1B**) showed that while the increase of signal amplitude during the cue/delay period relative to the fixation baseline was minimal, there was a differential activation between contralateral and ipsilateral instructed trials, and the modulatory effect of inactivation was consistent with another monkey, R (**Fig. S2**). Therefore, we used ROIs selected on the basis of "+contralateral saccade" contrast for a45 and FEF in monkey F.

Single-trial and per-session BOLD time-course analysis

For per-trial and per-session extraction of ROI BOLD signal amplitude, the 4D (x, y, z, time) volume time-courses from BrainVoyager QX VTC files were read in MATLAB and analyzed using custom software and BVQXtools v08d toolbox written by Jochen Weber (BrainInnovation).

Target configuration and eye movement behavior

We used an array of 18 possible targets (10°–16° eccentricity), 9 on the left and 9 on the right of the central fixation point. Targets and fixation point were 0.37° squares. The position of the eye was monitored in real-time and trials were aborted when the monkey did not fulfill fixation or instructed saccade reaction time (500 ms from the offset of the fixation point) criteria. The central fixation window radius was 3–4°, and the peripheral saccadic target window radius was 5–7°.

At 60 Hz sampling rate of video-based IR eye tracker, saccades of >0.33° amplitude could in principle be detected by a 20°/s velocity threshold. However, due to instrumental noise in the eye tracker, resulting in ~0.5° accuracy when the EPI sequence is running, we limited our analysis to saccades >1° that could be reliably identified using a combined velocity and acceleration algorithm. We also allowed transient eye position deflections (<250 ms) from the fixation window

to accommodate blinks that were inevitable during long fixation periods. During successful trials which were included in the fMRI analysis, both monkeys fixated within the prescribed window most of the 5 s delay period (>98%, monkey F; >94%, monkey R; with most deflections representing blinks). There was no difference in respect to within-window fixation durations between control vs. inactivation sessions, and left vs. right response trials ($p>0.05$ in all cases, except a small difference between instructed right and left trials in inactivation sessions in monkey R, 97% vs. 95%, $p=0.011$).

We next analyzed saccade frequency and directions during the delay period in specific trial types. Both monkeys held stable fixation (eye velocity <20°/s) for most part of the period: >78% in monkey R, and >83% in monkey F; the remaining were saccades or blinks exceeding 20°/s. There were small (<2%) differences in percent of stable fixation between some left and right response conditions, but these patterns were not consistent between monkeys. The saccade frequency, as well as the distribution of saccade directions across the 4 visual field quadrants in the 5 s delay period, were not significantly different between left and right response trials ($p>0.05$ in all cases, except for a difference between instructed right and left trials in monkey R), both in control and inactivation sessions. Both monkeys had slightly better fixation in inactivation sessions than in control sessions, in all spatial and instructed/choice conditions ($p<0.05$). The better fixation performance was also reflected in a lower blink frequency during inactivation, significant in all conditions in monkey R and in the left choice condition in monkey F, as well as in lower saccade frequency in left instructed and choice trials during inactivation in monkey R. One interpretation of these results is that monkeys were more "focused" or engaged in the task after inactivation, as they tried to cope with neural perturbations. Such increased alertness/effort could be a reason for generally increased activity in the frontal cortex after inactivation, as described below. However, the residual eye movements during the delay period are very unlikely the main source of spatially- and trial-specific cue/delay activity differences between control and inactivation sessions, since: 1) the eye movement differences were small 2) most eye movement patterns were inconsistent between monkeys, except better fixation in *all trial types* after inactivation; 3 there was always a reduced eye movement frequency in the inactivation sessions relative to control sessions, while the neural activity increased or decreased after inactivation depending on the trial type (e.g. decrease in left instructed trials but increase in left choice trials).

Abbreviations

BOLD, blood-oxygenation-level-depended; fMRI, functional magnetic resonance imaging; IHC, interhemispheric competition; LIP, lateral intraparietal area; FEF, frontal eye field; MT, middle temporal area; MST, middle superior temporal area; TPO, temporal parietal occipital area; Tpt, temporoparietal area; *as*, arcuate sulcus; *ips*, intraparetal sulcus; *sts*, superior temporal sulcus; GLM, general linear model; ERA, event-related average; HRF, hemodynamic response function

Supporting References

1. Xiang QS & Ye FQ (2007) Correction for geometric distortion and N/2 ghosting in EPI by phase labeling for additional coordinate encoding (PLACE). *Magn Reson Med* 57(4):731-741.
2. Kagan I, Iyer A, Lindner A, & Andersen RA (2010) Space representation for eye movements is more contralateral in monkeys than in humans. *Proc Natl Acad Sci U S A* 107(17):7933-7938.
3. Saleem K & Logothetis NK (2006) *A Combined MRI and Histology Atlas of the Rhesus Monkey Brain* (Academic Press, New York) p 336.